How to Cite:
Maheshna, N., Roopa, D., Karthick, R., Anandaram, H., Antony, J. P., Sangeetha, R. K., & Anusuya, M. (2022). Green synthesis of titanium dioxide nanoparticles and their multifaceted applications. *International Journal of Health Sciences*, *6*(S3), 5665–5680. https://doi.org/10.53730/ijhs.v6nS3.7210

Green synthesis of titanium dioxide nanoparticles and their multifaceted applications

Dr. N. Maheshna
Associate Professor of Civil Engineering in New Horizon College of Engineering, Bangalore, Karnataka, India

Dr. D. Roopa
Professor of Civil Engineering in New Horizon College of Engineering, Bangalore, Karnataka, India

Mr. R. Karthick
Assistant Professor of Physics in Periyar Maniammai Institute of Science & Technology, Thanjavur, Tamilnadu, India

Dr. Harishchander Anandaram
Assistant Professor of Centre for Excellence in Computational Engineering and Networking in Amrita Vishwa Vidyapeetham, Coimbatore, Tamilnadu, India

Mr. J. Prince Antony
Assistant Professor of Hotel Management in SRM Institute of Science & Technology, Triuchirapalli, Tamilnadu, India

Ms. R. K. Sangeetha
Assistant Professor of Physics in Sri Eshwar College of Engineering, Coimbatore, Tamilnadu, India

Dr. M. Anusuya
Professor of Physics and Registrar of Indra Ganesan Group of Institutions, Trichy, Tamilnadu, India
*Corresponding author email: sarananu94@gmail.com

***Abstract*---** Herein, we have prepared TiO2 photocatalyst using simple solution evaporation method for degradation of dye contaminant. The structural and optical possessions of the prepared photocatalyst have been categorized by a series of methods such as FTIR, XRD, SEM coupled with EDAX and UV-DRS. The photocatalytic activity of the obtained TiO2 nanoparticles were investigated by monitoring the

degradation of solution of Methylene Blue (MB) as model dye molecule, using simulated solar irradiation. Photo-degradation experimental results point out that the prepared TiO2 photocatalyst exhibits advanced photocatalytic action over commercially available powder TiO2. The bacterial activity of TiO2 nanoparticles monitored by using E.coli and S.aureus bacterial strains. The antimicrobial activity of the synthesized sample shows a good result against gram positive bacteria. The synthesized nano materials have great prospective to contribute in the wastewater treatment and bio-medical management technologies.

***Keywords*---** TiO2, dye degradation, photocatalytic dye degradation, Tulsi, antibacterial activity.

Introduction

Dyes are major coloring material which are widely used in the field of textile industries, medicine, food and cosmetics etc. (Slama 2021, Wargala 2021, Ma 2022). On considering its industrial application these dyes are directly released in to the aquatic environment which cause threats to human life (Sharma 2021). Dyes are alienated into three partitions namely (i) anionic (ii) cationic and (iii) non-ionic. Among them cationic dyes are used in larger industrial application such as food coloring, medicine and textile application. When these cationic dyes are directly released in to the aquatic system, which cause poisoning to the aquatic life by blocking sunlight and decreases the aquatic photosynthesis. When these dye contaminated water are utilized by human, which cause vomiting, carcinogenic, kidney failure and eye irritation etc. (Slama 2021). Several methods such as flocculation, adsorption, catalytic removal, filtration etc., are used for the removal of this dye stuff. Among them photocatalytic dye removal plays a major role because of its easy synthesis, cheap and highly efficient (Din 2021). Materials which are used widely Nanotechnology has attracted assortment of consideration due to its gigantic applications in practically every industry, from textiles to medical, including electronics (Rao 2015).

Nanomaterials are materials with a nanoscale scale in at least one dimension and significant changes in characteristics that can be used in a variety of applications. IT sector, energy, environment, aeronautics, medicine, nanoscience and biotechnology are among them nanoscience and nanotechnology have been extensively used (Vani 2017). To produce smaller-sized nanoparticles, several chemical methods are adopted for the synthesize of metal oxide nanoparticles are hydrothermal, sol-gel, co-precipitation, and solvothermal techniques are being used extensively (Pudukudy 2017, Ding 2001, Rao 2014, Aslani 2011). However, when using these nanoparticles for biological applications, the toxicity of these chemically produced TiO2 nanoparticles is a major stumbling block (Mangalampalli 2019). In order to use TiO2 nanoparticles in biological applications, biological processes are used to produce less or non-toxic

TiO2 nanoparticles. TiO2 nanoparticles are biosynthesized by algae (El-Sayyad 2018) but the time taking reaction and less availability of the microorganisms are restrict for major biological application. Along with their profuse availability, hasty synthesis, and prospective to create smaller stable nanoparticles, plant extracts with phytochemicals, notably from leaves, are often employed to construct TiO2 nanoparticles (Raliya 2014, Sharma 2017, Suresh 2018, JohnSushma 2016).

TiO2 nanoparticle was applied in variety of application including skin care lotions, food colorants, inks, toothpaste, and so on. By lowering the band gap these TiO2 nanoparticles can be implemented as a photocatalytic material for the degradation of several organic compounds even up to higher extent. When TiO2 is exposed to UV/Visible light, it produces more active species for organic molecule breakdown. Phytogenic synthesis of TiO2 nanoparticles has attracted a lot of interest, because of its easy and environmentally friendly synthesis process (Shanavas 2020).

Ocimum sanctum (Tulsi) is a therapeutic basil that is extensively consumed in Asian continent, Africa, and Arabic countries (Mondal 2009). Ocimum sanctum leaves have long been used to treat a variety of infectivity. Ocimum sanctum belongs to the family Lamiaceae and it has variety of chemical compound such as oleanolic acid, ursolic acid, rosmarinic acid, eugenol, carvacrol, linalool, and β- caryophyllene are identified in its leaf phytochemical morphology (Sundaram 2012, Das2006). Apsana et al. suggested that the the reductions of Ca and Co metal ions by leaf extract is due to the presence of phenolic eugenol matrix. Apsana et al, proposed that the SrO NPs are synthesized using microwave green chemical method shows a better antibacterial activity. (Apsana 2017).

T. Pushpamalani et al, synthesised TiO2 nanoparticle using from Piper betel (PB), Ocimum tenuiflorum (OT), Moringa oleifera (MO), and Coriandrum sativum (CS) and he concluded that Moringa oleifera extract acted as a superior reducing agent and exhibited better photocatalytic degradation efficiency against Malachite green dye (Pushpamalini, 2021). ZnO nanoparticles were produced from Ocimum basilicum plant extract that successfully slow down pathogenic microbial strains of clinical source (Irshad 2020). Biswajit Saha et al prepared silver and TiO2 nano particles from Tulsi leaf extract (Saha 2019). Herein, we used Ocimum basilicum leaf extract were used for the production of TiO2 nano particles. The obtained nano particles are characterized using FTIR, SEM, EDAX and XRD analysis. In addition, TiO2 nanoparticles bacterial and catalytic strength were examined by S.aureus, E.coli and MB dye respectively.

Materials and Methods

Materials

The plant compounds (Ocimum Basilicum leaf) were collected from Local mark at Tirunelveli, Tamilnadu, India. The source material of Titanium

(IV) isopropoxide (Merck 99 % purity) were processed by double distilled water.

Preparation of Ocimum basilicum leaf extract

A fresh Ocimum basilicum leaves was washed repeatedly with demineralized water in room temperature for 24 hrs. About 500 mg of Ocimum basilicum leaves added to 200 mL distilled water in 500 mL beaker and boiled at a temperature of 100 °C for one hr. The leaf aliquot was filter and collected for supplementary investigation.

Synthesis ofTiO2 nanoparticles

About, 1 M of Titanium Tetra Isopropoxide was added to the 250 ml beaker containing in 20 mL Ocimum basilicum leaf extract and stirred at the temperature of 60°C for 4 hrs. Subsequently, at the end of reaction, the whole solution is centrifuged at 12000 rpm for 600 seconds. Then the centrifuged TiO2 particles were washed continuously with ethanol and centrifuges for 8000 rpm for 300 seconds. Finally, the separated TiO2 nanoparticles were calcinated at 500°C in furnace at a ramp of 5 °C/ min for about 3 hours. The sintered titanium dioxide nano powder was used for further analytical techniques.

Characterization of TiO2 photocatalyst

X-ray diffraction (XRD) patterns were verified using (PANalytical B.V., Netherlands). Fourier transform infrared (FT-IR) spectra of composite were measured using (Perkin elmer) by powder sample technique ranging from 400 to 4000 cm-1. The surface morphology of composite sample was examined by scanning electron microscopy (SEM) coupled with EDAX with an accelerating voltage of 30 kV (Carl Zeiss). Ultraviolet−visible (UV−vis) diffused reflectance spectra were measured on a spectrophotometer (UV-2700, Shimadzu) using BaSO4 as standard.

Photocatalytic dye degradation activity

The photocatalytic degradation of MB dye TiO2 photocatalyst using simulated solar irradiation. To carry out the reaction at first 50 ml of MB dye solution (1 X 10-5 M) was taken in a 250 mL beaker. The space between the simulate light and dye solution is approximately 10 cm. About 0.05 gram of photo catalyst was mixed to the dye solution and kept dark for 2 hrs to reach the adsorption-desorption equilibrium. After the attainment of equilibrium, the solution was continuous stirring with the 550 rpm and placed in simulated solar simulator. Then the aliquot solution was collected over every 10 min time interval, centrifuge and degradation of dye was measured using absorbance value of MB using spectrophotometer. The removal % of the dye molecule was determined using following calculation.

Percentage of dye degradation = (CMBi- CMBT/CMBi)X 100

Where,
CMBi= Initial dye concentrations.
CMBT = Concentration of dye solution at time interval 't'.

Anti-bacterial activity

The disk diffusion method is used to evaluate antimicrobial susceptibility of Ocimum basilicum leaf and TiO2 nanoparticles. Antibacterial properties of tulsi extract and TiO2 nanoparticles was tested against gram-negative and gram-positive bacteria such as E.coli and S.aureus as selected model bacterium. In order to prepare nutrient agar plate all, the glassware's are sterilized in 120o C in autoclave at 30 min. Cork borer is used to dig a well over the Petri plate and circular discs impregnated with 100µL of synthesized TiO2 nanoparticle and Ocimum basilicum leaf were placed in the well of the petri plates. The inoculated plates with sample were incubated at 40 o C for 24 h. After 24 hrs of incubation period at 35°C the Zones of inhibition were measured. After the completion of incubation period, all plates have revealed the Zone of Inhibitions (ZOI) are measured using ruler in mm scale.

Results and discussions

XRD analysis

The XRD pattern of the prepared TiO2 photocatalyst sample are shown in figure 1. The diffraction peaks such as (101), (004), (200), (105), (211), (204), (118), and (315) are identified to corresponding crystal planes of the powder TiO2 are accordance with the JCPDS card no (21-1272) (Pookmanee 2010). The obtained diffractions peak are well defined inclines to the anatase phase of TiO2. For water purification process and dye removal, these anatase phase are very acquainted (Lebedev 2018). The size of TiO2 photocatalyst is 24 nm were calculated from Debye Scherrer formula. The pure anatase phase implies that the XRD pattern has no other impurities related to the rutile phase indicating the sample purity.

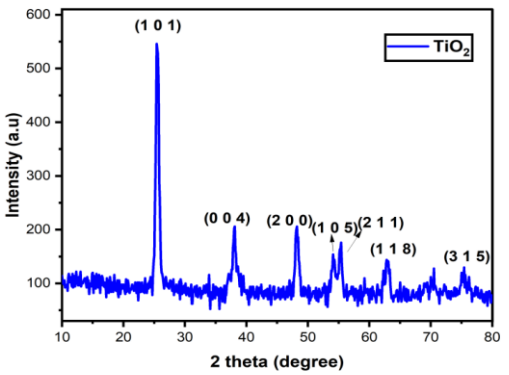

Figure 1. XRD spectrum of synthesized TiO2 particle

FTIR analysis

The biosynthesized TiO2 nanoparticles have relevant functional groups, the chemical skeleton was characterized using FTIR spectroscopy. The FTIR spectrum of produced TiO2 photocatalytic nanoparticle are exposed in figure 2. The band 3415 cm−1 and 1631 cm−1 were indexed to the both asymmetric and symmetric stretching vibrations of hydroxyl (O–H) group delivers the presence of moisture in the sample (Kumar 2000). The band approximately at 712 cm−1 is the characteristic peak of O-Ti bond and Ti-O-Ti bond in the TiO2 matrix (Al-Amin 2016). The weak bands around 2930 cm−1 and 2852 cm−1 match to the vibrational modes of O–H, RCOO− and C-C groups present in the prepared TiO2 sample indicate the incomplete removal of these groups during ethyl alcohol and demineralized water washing. Similarly, the peaks at 1384 cm−1 could be attributed to C=O and –CH2- groups which are present in the synthesized TiO2 nanoparticles.

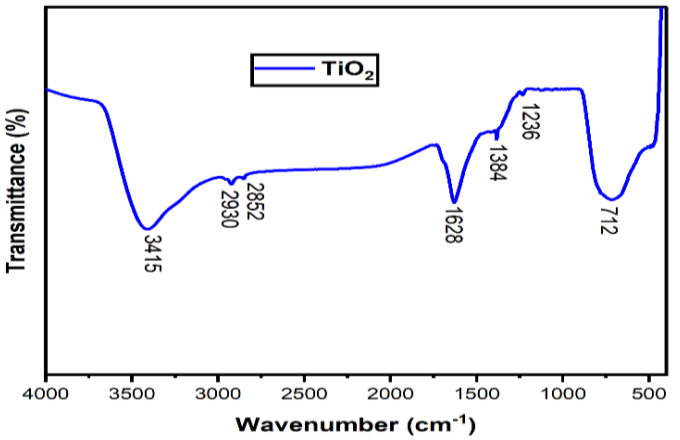

Figure 2. FTIR spectrograph of synthesized TiO2 particle

UV-DRS analysis

For photocatalytic material optical absorption properties is a vital factor for determination of material photoactive nature. The absorption spectra and bandgap energy spectra of TiO2 disclosed in figure 3 (a-b). The UV region absorption of TiO2 nanoparticles expressed an excited charge carriers in 2-p state. The direct bandgap energy value for the synthesized TiO2 photocatalyst calculate from the suggested tauc plot method. Herein the synthesized composite shows a reduced bandgap value of 3.15 eV than the commercial TiO2 3.23 eV (Wan 2007) indicates the improved light absorption properties with heightened conductivity. Hence, the prepared TiO2 photocatalyst can be explored for the use of visible light photo catalysis.

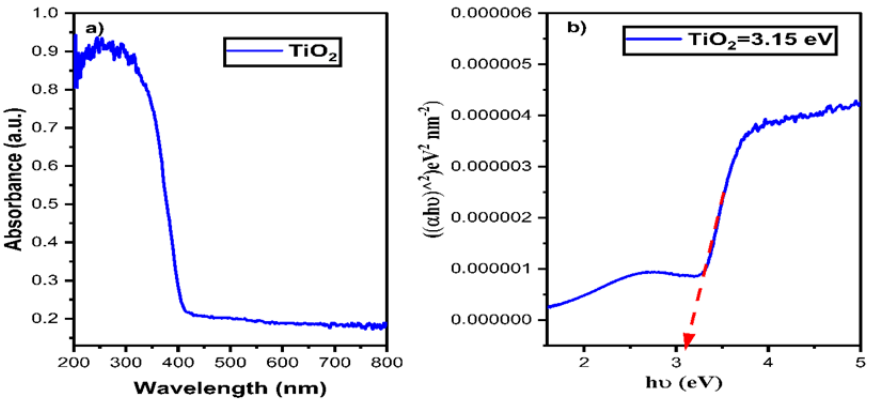

Figure 3. (a-b): (a) UV-DRS and (b) Bandgap spectrum of synthesized TiO2 particle

SEM with EDX analysis

The representative SEM images of TiO2 nanoparticles are shown in figure 4 (a–b), respectively, for a higher(a) and a lower (b) magnification. Figure 4 (a-b) express that spherical aggregated particle TiO2 particles with smooth surface to form larger particles observed in both lower and magnifications. The large aggregative particles are observed from the existing plant nutrients. Due to the presence of plant compounds the particles are aggregated and shuffled with each other. The existing plant nutrients and their stretched molecules were analyzed from FTIR analysis. The EDX spectral of investigated TiO2 samples have exposed peaks of Ti and O elements are shown in figure 4(c). The presence of Ti (42.79) and O (57.21) atomic weight percentage in figure 4 (d) is substantiates the formation of pure TiO2 with no other impurities which is accordance with the both XRD and FTIR result.

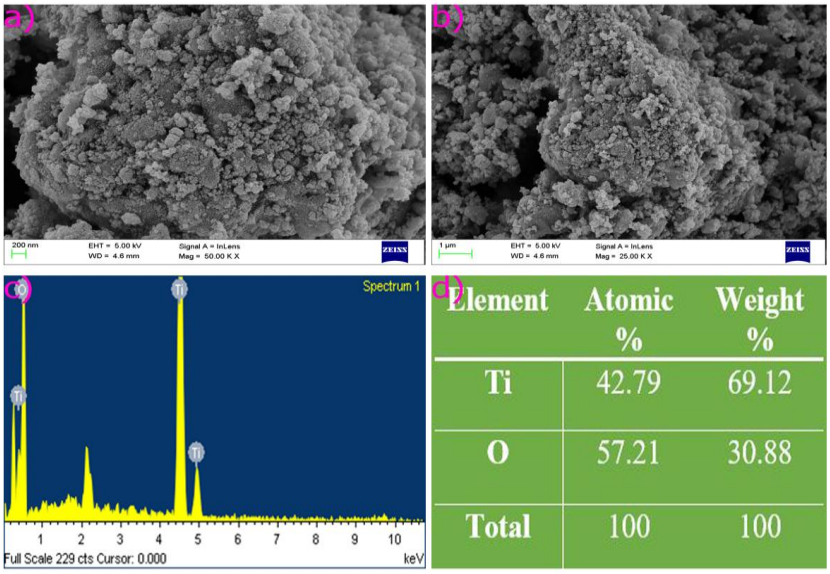

Element	Atomic %	Weight %
Ti	42.79	69.12
O	57.21	30.88
Total	100	100

Figure 4. (a-b) SEM images, (c) EDX spectrum and table (d) of synthesized TiO2 particle

Photocatalytic activity

The photocatalytic activity of TiO2 nanoparticles over cationic methylene blue dye were depicts in under simulated solar irradiation for 120 min shown in figure 5(a). represents the percentage of MB dye removal under murky and illumination conditions using photo catalyst TiO2. The dual action of photocatalytic TiO2 such as adsorption followed photocatalytic removal of MB dye happened. From figure 5(a) which clearly convey that the photocatalytic removal percentage is high and adsorption percentage is minimal is due to the less adsorption site in TiO2 photocatalyst. The kinetic study reviles the discoloration of MB follow the k app the first-order kinetics using straight line shown in figure 5 (b-c) by plotting time of irradiation vs ln C/C0. The rate constant of the apparent rate constant of dye molecule under the influence simulated solar light irradiation is analyzed from using the below formula (Dung 2005).

$$\ln C0/C = kapp.t$$

The kinetic rate constants were deliberate to be 0.0134 min−1 for commercial TiO2 nanoparticles and 0.02414 min−1 for our TiO2 catalysts, respectively. The prepared TiO2 surface has crystalline phase of anatase which is considered a potential candidate for the destroy of various colored stains. The present research work compared with previous reported work and tabulated in table 1. After the achievement adsorption-desorption kinetic equilibrium conditions the initiation of photolysis process starts at the exposure of simulated solar irradiation. During photocatalytic degradation period of MB molecules degraded by the simulation of oxidation reduction caused by the surface contact of TiO2

catalyst further it promotes the photo generated hole and OH radicals to the MB molecules. The formation of VB h+ in the valence band and CB (e−) in the conduction band are usually concomitant with revelation of TiO2 surface by simulated light energy. These generated electrons readily react with water molecules to produces a sequence of highly reactive radical species (OH-)and (•O2-) which are involve for further fragmentation of huge amount of MB molecule (Yin 2006, Jimmy 2006) which are revealed in figure 6.

The photocatalytic degradation efficiency was 94% during the first cycle are shown in figure 5(d). The catalyst activity slightly decreases in alternative cycle 2, 3, 4 and 5, producing 92%, 91%, 90% and 88% dye degradation efficiency. The deactivation of the photo catalyst is due to the adsorbed intermediates causing surface poisoning of system (Abdelaal 2013).

$$TiO2 + h\nu \rightarrow TiO2.VBh^{+} + TiO2C.B(e^{-})$$

$$TiO2V.B\ (h^{+}) + H2O \rightarrow TiO2 + H^{+} + OH^{-}(Radicle)$$

$$TiO2C.B\ (e^{-}) + OH^{-} \rightarrow TiO2^{+}.OH$$

$$TiO2h^{+} + O2 \rightarrow \cdot O2$$

$$O2\cdot + OH/h^{+} + C16H18ClN3S\cdot^{+} \rightarrow \text{Degradation products} + H2O + CO2$$

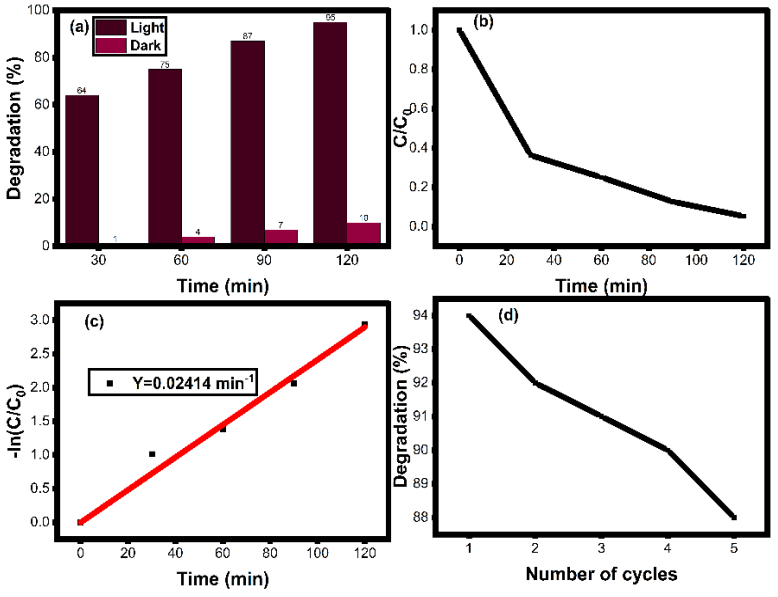

Figure 5. (a-d). (a) photocatalytic MB dye degradation efficiency, (b) C/C0, (c) lnC/C0 vs Time and (d) reusability study of TiO2 particle

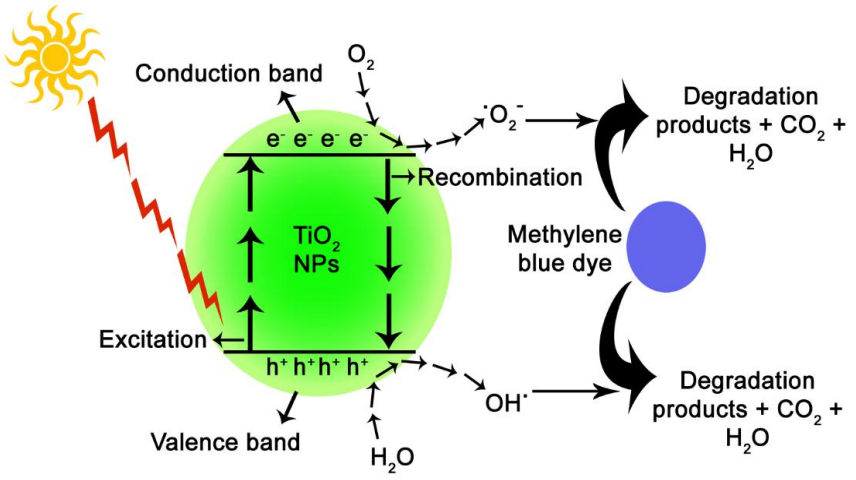

Figure 6. Schematic diagram of MB dye degradation mechanism

Comparison with collected works results

S.No	Catalyst	Pollutant	Dye/Catalyst Dosage	Irradiation Source	Efficiency	Ref
1.	RGO/TiO2	Diphenhydramine (DP) And Methyl Orange	7.5 mL/1.0 g L−1	Mercury	94%	Pastrana 2012
2.	Sn/TiO2	Malachite Green	25 ml	UV	90%	Sayılkan 2007
3.	Pd/TiO2	Methylene Blue	0.75 g /500 ml	Xenon 300 W	99.5%	Abdelaal 2013
4.	CeO2/TiO2	Bromophenol Dye		Xenon 300W	72%	Ameen 2014
5.	TiO2 nanotubes	Indigo Carmine	100 ml / 0.1 g/L	Mercury 125W	90%	Costa 2009
6.	TiO2/C	Blue QR 19	200 /50 mg	Mercury 125 W	89%	da Costa 2013
7.	Ag-coated Ni@TiO2	Crystal Violet	20 mL/10 mg	Hg lamp20W	80%	Ding 2014
8.	TiO2	Methyl Orange	50mL	Xenonlamp150W	80%	Han 2010
9.	RuO2/SiO2 /TiO2	Methyl Orange	4 ml	F15 W/T8 UV	98%	Ibhadon 2008
10.	CNT/TiO2	Methyl Orange	1000mL/200 mg	Mercury300 W	94%	Jiang 2013
11.	TiO2	Methylene blue	50 ml/0.05mg	Xenon arc lamp	95%	Current work

Antimicrobial Activity

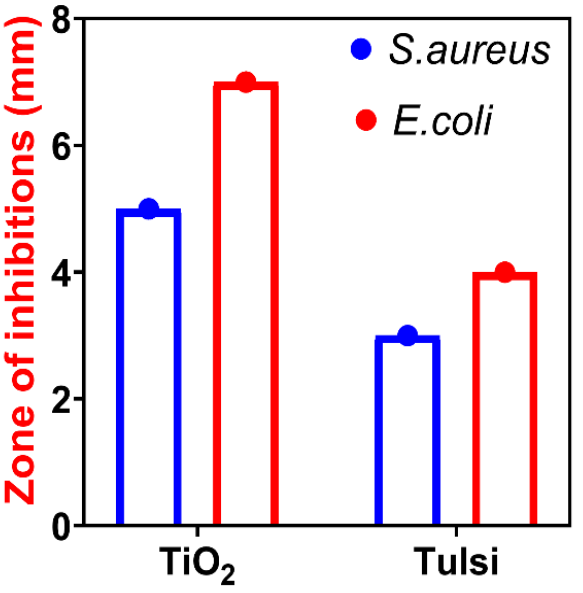

Figure 7. Antibacterial activity of TiO2 nanoparticles and Ocimum basilicum leaf extract over gram-positive and gram-negative bacteria

The synthesized TiO2 nanoparticles and Ocimum basilicum leaf extract has tested with microbial species, namely, S. aureus and E. coli are revels in figure 7. The Ocimum basilicum leaf extract and synthesized TiO2 exhibited significant antimicrobial activity against E. coli (4 mm) and (7.8 mm) and S. aureus (3.5mm) and (5 mm). On measuring the inhibition zone of plates, the maximum inhibitions zone was produced by TiO2 particle over E. coli (7.8 mm) bacterium. The triplicate number of tests are conducted. The mechanism of this well-developed antibacterial activity is due to the action of produced TiO2 generated hydroxyl groups and Reactive Oxygen Species (ROS), which are capable of melt the cell wall lead phospholipid peroxidation of bacteria leads to the death (Xiao 2015, Schieber 2014, Dowd 2021). In this report, TiO2 nanoparticles establish to be a successful antimicrobial drug which can be lead for the progression of new antimicrobial drugs and antimicrobial agents.

Conclusion

In summary, a simple and profitable route was used for synthesis of TiO2 nanoparticles via green synthesis. In the current study, the TiO2 nanoparticles were blended from Titanium tetra isoproxide using Ocimum basilicum leaf extract by using solvo-thermal scheme From SEM analysis, the TiO2 nanoparticles were found to be spherical in shape with aggregated morphology. FTIR results confirms the purity of TiO2 nanoparticles. The synthesized TiO2 nanoparticles was found to be the

superlative photocatalytic degradation activity over MB dye. Finally, TiO2 nanoparticles exhibited potential candidate for degradation of methylene blue under simulated solar irradiation and possess high activity against gram positive bacteria. The present outcome proposed that the TiO2 nanoparticles shows an effective photocatalytic agent for remediation of pollutant from various dye-based industries.

Conflict of interest

The authors have no conflict of interest

References

1. Slama, H. B., ChenariBouket, A., Pourhassan, Z., Alenezi, F. N., Silini, A., Cherif-Silini, H., &Belbahri, L. (2021). Diversity of synthetic dyes from textile industries, discharge impacts and treatment methods. Applied Sciences, 11(14), 6255.
2. Wargala, E., Sławska, M., Zalewska, A., & Toporowska, M. (2021). Health Effects of Dyes, Minerals, and Vitamins Used in Cosmetics. Women, 1(4), 223-237.
3. Ma, X., Shi, L., Zhang, B., Liu, L., Fu, Y., & Zhang, X. (2022). Recent advances in bioprobes and biolabels based on cyanine dyes. Analytical and Bioanalytical Chemistry, 1-23.
4. Sharma, J., Sharma, S., &Soni, V. (2021). Classification and impact of synthetic textile dyes on Aquatic Flora: A review. Regional Studies in Marine Science, 45, 101802.
5. Slama, H. B., ChenariBouket, A., Pourhassan, Z., Alenezi, F. N., Silini, A., Cherif-Silini, H., &Belbahri, L. (2021). Diversity of synthetic dyes from textile industries, discharge impacts and treatment methods. Applied Sciences, 11(14), 6255.
6. Din, M. I., Khalid, R., Najeeb, J., & Hussain, Z. (2021). Fundamentals and photocatalysis of methylene blue dye using various nanocatalytic assemblies-a critical review. Journal of Cleaner Production, 298, 126567.
7. Rao, K. G., Ashok, C. H., Rao, K. V., Chakra, C. S., &Tambur, P. (2015). Green synthesis of TiO2 nanoparticles using Aloe vera extract. Int. J. Adv. Res. Phys. Sci, 2(1A), 28-34.
8. Vani, P., Manikandan, N., &Vinitha, G. (2017). A green strategy to synthesize environment friendly metal oxide nanoparticles for potential applications: A review. Asian J. Pharm. Clin. Res, 10, 337.
9. Pudukudy, M., Yaakob, Z., Mazuki, M. Z., Takriff, M. S., &Jahaya, S. S. (2017). One-pot sol-gel synthesis of MgO nanoparticles supported nickel and iron catalysts for undiluted methane decomposition into COx free hydrogen and nanocarbon. Applied Catalysis B: Environmental, 218, 298-316.
10. 10.Ding, Y., Zhang, G., Wu, H., Hai, B., Wang, L., & Qian, Y. (2001). Nanoscale magnesium hydroxide and magnesium oxide powders: control over size, shape, and structure via hydrothermal synthesis. Chemistry of materials, 13(2), 435-440.

11. Rao, K. G., Ashok, C. H., Rao, K. V., & Chakra, C. S. (2014). Structural properties of MgO nanoparticles: synthesized by co-precipitation technique. International Journal of Science and Research, 3(12), 43-46.
12. Aslani, A., Arefi, M. R., Babapoor, A., Amiri, A., &Beyki-Shuraki, K. (2011). Solvothermal synthesis, characterization and optical properties of ZnO, ZnO–MgO and ZnO–NiO, mixed oxide nanoparticles. Applied Surface Science, 257(11), 4885-4889.
13. Mangalampalli, B., Dumala, N., & Grover, P. (2019). Toxicity assessment of magnesium oxide nano and microparticles on cancer and non-cancer cell lines. The Nucleus, 62(3), 227-241.
14. El-Sayyad, G. S., Mosallam, F. M., & El-Batal, A. I. (2018). One-pot green synthesis of magnesium oxide nanoparticles using Penicilliumchrysogenum melanin pigment and gamma rays with antimicrobial activity against multidrug-resistant microbes. Advanced Powder Technology, 29(11), 2616-2625.
15. Raliya, R., Tarafdar, J. C., Choudhary, K., Mal, P., Raturi, A., Gautam, R., & Singh, S. K. (2014). Synthesis of MgO nanoparticles using Aspergillus tubingensis TFR-3. Journal of Bionanoscience, 8(1), 34-38.
16. Sharma, G., Soni, R., &Jasuja, N. D. (2017). Phytoassisted synthesis of magnesium oxide nanoparticles with Swertiachirayaita. Journal of Taibah University for Science, 11(3), 471-477.
17. Suresh, J., Pradheesh, G., Alexramani, V., Sundrarajan, M., & Hong, S. I. (2018). Green synthesis and characterization of hexagonal shaped MgO nanoparticles using insulin plant (Costuspictus D. Don) leave extract and its antimicrobial as well as anticancer activity. Advanced Powder Technology, 29(7), 1685-1694.
18. JohnSushma, N., Prathyusha, D., Swathi, G., Madhavi, T., Deva Prasad Raju, B., Mallikarjuna, K., & Kim, H. S. (2016). Facile approach to synthesize magnesium oxide nanoparticles by using Clitoriaternatea—characterization and in vitro antioxidant studies. Applied Nanoscience, 6(3), 437-444.
19. Shanavas, S., Priyadharsan, A., Karthikeyan, S., Dharmaboopathi, K., Ragavan, I., Vidya, C., &Anbarasana, P. M. (2020). Green synthesis of titanium dioxide nanoparticles using Phyllanthusniruri leaf extract and study on its structural, optical and morphological properties. Materials Today: Proceedings, 26, 3531-3534.
20. Mondal, S., Mirdha, B. R., &Mahapatra, S. C. (2009). The science behind sacredness of Tulsi (Ocimum sanctum Linn.). Indian J PhysiolPharmacol, 53(4), 291-306.
21. Sundaram, R. S., Ramanathan, M., Rajesh, R., Satheesh, B., &Saravanan, D. (2012). LC-MS quantification of rosmarinic acid and ursolic acid in the Ocimum sanctum Linn. leaf extract (Holy basil, Tulsi). Journal of Liquid Chromatography & Related Technologies, 35(5), 634-650.

22. Das, S. K., &Vasudevan, D. M. (2006). Tulsi: The Indian holy power plant.
23. Apsana, G., George, P. P., &Devanna, N. (2017). Green synthesis and thermo, optical properties of M2P2O7 [M= Ca and Co] nanoparticles. Inter. J. Pharma. BioSci, 8, 148..
24. Pushpamalini, T., Keerthana, M., Sangavi, R., Nagaraj, A., &Kamaraj, P. (2021). Comparative analysis of green synthesis of TiO2 nanoparticles using four different leaf extract. Materials Today: Proceedings, 40, S180-S184.
25. Irshad, S., Riaz, M., Anjum, A. A., Sana, S., Saleem, R. S. Z., &Shaukat, A. (2020). Biosynthesis of ZnO nanoparticles using Ocimumbasilicum and determination of its antimicrobial activity. J Anim Plant Sci, 301, 185-191.
26. Saha, B., Kumar, S., &Sengupta, S. (2019). Green synthesis of nano silver on TiO2 catalyst for application in oxidation of thiophene. Chemical Engineering Science, 199, 332-341.
27. Pookmanee, P., Kuntatun, T., Kangwansupamonkon, W., &Phanichphant, S. (2010). Titanium dioxide powder prepared by a low temperature hydrothermal method. In Advanced Materials Research (Vol. 93, pp. 627-630). Trans Tech Publications Ltd.
28. Lebedev, A., Anariba, F., Tan, J. C., Li, X., & Wu, P. (2018). A review of physiochemical and photocatalytic properties of metal oxides against Escherichia coli. Journal of Photochemistry and Photobiology A: Chemistry, 360, 306-315.
29. Kumar, P. M., Badrinarayanan, S., &Sastry, M. (2000). Nanocrystalline TiO2 studied by optical, FTIR and X-ray photoelectron spectroscopy: correlation to presence of surface states. Thin solid films, 358(1-2), 122-130.
30. Al-Amin, M., Dey, S. C., Rashid, T. U., Ashaduzzaman, M., &Shamsuddin, S. M. (2016). Solar assisted photocatalytic degradation of reactive azo dyes in presence of anatase titanium dioxide. Int. J. Latest Res. Eng. Technol, 2(3), 14-21.
31. Wan, L., Li, J. F., Feng, J. Y., Sun, W., & Mao, Z. Q. (2007). Anatase TiO2 films with 2.2 eV band gap prepared by micro-arc oxidation. Materials science and engineering: B, 139(2-3), 216-220.
32. Dung, Nguyen Thi, Nguyen Van Khoa, and Jean-Marie Herrmann. "Photocatalytic degradation of reactive dye RED-3BA in aqueous TiO2 suspension under UV-visible light." International Journal of Photoenergy 7.1 (2005): 11-15..
33. Photocatalytic degradation of methylene blue dye over novel spherical mesoporous Cr2O3/TiO2 nanoparticles prepared by sol-gel using octadecylamine template.
34. Yin, J. B., & Zhao, X. P. (2006). Enhanced electrorheological activity of mesoporous Cr-doped TiO2 from activated pore wall and high surface area. The Journal of Physical Chemistry B, 110(26), 12916-12925.
35. Jimmy, C. Y., Li, G., Wang, X., Hu, X., Leung, C. W., & Zhang, Z. (2006). An ordered cubic Im 3 m mesoporous Cr–TiO 2 visible light photocatalyst. Chemical communications, (25), 2717-2719.

36. Abdelaal, M. Y., & Mohamed, R. M. (2013). Novel Pd/TiO2 nanocomposite prepared by modified sol–gel method for photocatalytic degradation of methylene blue dye under visible light irradiation. Journal of Alloys and Compounds, 576, 201-207.
37. Pastrana-Martínez, L. M., Morales-Torres, S., Likodimos, V., Figueiredo, J. L., Faria, J. L., Falaras, P., & Silva, A. M. (2012). Advanced nanostructured photocatalysts based on reduced graphene oxide–TiO2 composites for degradation of diphenhydramine pharmaceutical and methyl orange dye. Applied Catalysis B: Environmental, 123, 241-256.
38. Sayılkan, F., Asiltürk, M., Tatar, P., Kiraz, N. A. D. İ. R., Arpac, E. R. T. U. Ğ. R. U. L., &Sayılkan, H. (2007). Photocatalytic performance of Sn-doped TiO2 nanostructured mono and double layer thin films for Malachite Green dye degradation under UV and vis-lights. Journal of Hazardous Materials, 144(1-2), 140-146.
39. Abdelaal, M. Y., & Mohamed, R. M. (2013). Novel Pd/TiO2 nanocomposite prepared by modified sol–gel method for photocatalytic degradation of methylene blue dye under visible light irradiation. Journal of Alloys and Compounds, 576, 201-207.
40. Ameen, S., Akhtar, M. S., Seo, H. K., & Shin, H. S. (2014). Solution-processed CeO2/TiO2 nanocomposite as potent visible light photocatalyst for the degradation of bromophenol dye. Chemical Engineering Journal, 247, 193-198.
41. Costa, L. L., & Prado, A. G. (2009). TiO2 nanotubes as recyclable catalyst for efficient photocatalytic degradation of indigo carmine dye. Journal of Photochemistry and Photobiology A: Chemistry, 201(1), 45-49.
42. da Costa, E., Zarbin, A. J., & Peralta-Zamora, P. (2013). Multivariate optimisation of TiO2/carbon nanocomposites for photocatalytic degradation of a reactive textile dye. Materials research bulletin, 48(2), 581-586.
43. Ding, Q., Zhang, L., & Yang, L. (2014). A simple approach for the synthesis of Ag-coated Ni@ TiO2 nanocomposites as recyclable photocatalysts and SERS substrate to monitor catalytic degradation of dye molecules. Materials Research Bulletin, 53, 205-210.
44. Han, H., & Bai, R. (2010). Highly effective buoyant photocatalyst prepared with a novel layered-TiO2 configuration on polypropylene fabric and the degradation performance for methyl orange dye under UV–Vis and Vis lights. Separation and Purification Technology, 73(2), 142-150.
45. Ibhadon, A. O., Greenway, G. M., & Yue, Y. (2008). Photocatalytic activity of surface modified TiO2/RuO2/SiO2 nanoparticles for azo-dye degradation. Catalysis Communications, 9(1), 153-157.
46. Jiang, T., Zhang, L., Ji, M., Wang, Q., Zhao, Q., Fu, X., & Yin, H. (2013). Carbon nanotubes/TiO2 nanotubes composite photocatalysts for efficient degradation of methyl orange dye. Particuology, 11(6), 737-742.
47. Xiao, G., Zhang, X., Zhang, W., Zhang, S., Su, H., & Tan, T. (2015). Visible-light-mediated synergistic photocatalytic antimicrobial

effects and mechanism of Ag-nanoparticles@ chitosan–TiO2 organic–inorganic composites for water disinfection. Applied Catalysis B: Environmental, 170, 255-262.
48. Schieber, M., &Chandel, N. S. (2014). ROS function in redox signaling and oxidative stress. Current biology, 24(10), R453-R462.
49. Dowd, K., Nair, K. M., & Pillai, S. C. (2021). Photocatalytic degradation of antibiotic-resistant genes and bacteria using 2D nanomaterials: What is known and what are the challenges?. Current Opinion in Green and Sustainable Chemistry, 30, 100471.